

Onset of aseismic creep on major strike-slip faults

Ziyadin Çakir^{1,2*}, Semih Ergintav^{2*}, Haluk Özener^{3*}, Uğur Dogan^{4*}, Ahmet M. Akoglu^{5*}, Mustapha Meghraoui^{6*}, and Robert Reilinger^{7*}

¹Istanbul Technical University, Department of Geology, 34469, Maslak, Istanbul, Turkey

²TÜBİTAK Marmara Research Center, Earth and Marine Sciences Institute, 41470, Gebze, Izmit, Turkey

³Boğaziçi University, Kandilli Observatory, 34680, Çengelköy, Istanbul, Turkey

⁴Yıldız Teknik University, Department of Geomatics, 34220, Esenler, Istanbul, Turkey

⁵King Abdullah University of Science and Technology (KAUST), 23955-6900, Thuwal, Saudi Arabia

⁶Institut de Physique du Globe de Strasbourg (IPGS), UMR 7516, 5 rue René Descartes, 67084 Strasbourg, France

⁷Massachusetts Institute of Technology, Department of Earth, Atmospheric, and Planetary Sciences, 77 Massachusetts Avenue, Cambridge, Massachusetts 02139, USA

ABSTRACT

Time series analysis of spaceborne synthetic aperture radar (SAR) data, GPS measurements, and field observations reveal that the central section of the Izmit (Turkey) fault that slipped with a supershear rupture velocity in the A.D. 1999, M_w 7.4, Izmit earthquake began creeping aseismically following the earthquake. Rapid initial postseismic afterslip decayed logarithmically with time and appears to have reached a steady rate comparable to the pre-earthquake full fault-crossing rate, suggesting that it may continue for decades and possibly until late in the earthquake cycle. If confirmed by future monitoring, these observations identify postseismic afterslip as a mechanism for initiating creep behavior along strike-slip faults. Long-term afterslip and/or creep has significant implications for earthquake cycle models, recurrence intervals of large earthquakes, and accordingly, seismic hazard estimation along mature strike-slip faults, in particular for Istanbul which is believed to lie adjacent to a seismic gap along the North Anatolian fault in the Sea of Marmara.

INTRODUCTION

Understanding the behavior of active faults in response to tectonic stresses is a critical issue in earthquake physics and seismic hazard assessments (Carpenter et al., 2011). While most active faults are unstable and move abruptly, releasing in seconds to a few minutes the strain accumulated around them for decades to centuries, some faults slip continuously, storing little or no strain and are therefore considered to be unlikely to produce significant earthquakes as long as this behavior persists (Bürgmann et al., 2000). Although aseismic fault creep was first reported over half a century ago along some major plate boundary faults, including the San Andreas fault in California (United States) and the North Anatolian fault in Turkey, the origin and physical processes of fault creep remain subjects of debate (Schleicher et al., 2010). Two primary, complementary, and competing mechanisms have been proposed to explain the mechanics of aseismic fault creep: (1) the presence of weak mineral phases such as clay and phyllosilicates in the bulk composition of fault zones (Carpenter et al., 2011) or the formation of highly localized, phyllosilicate-rich interconnected networks of shear planes or foliations (Colletini et al., 2009) via chemical and mechanical processes, and/or (2) trapped fluid overpressures within fault zones (Byerlee, 1990). Although recent observa-

tions (Lockner et al., 2011) support the idea that aseismic creep is controlled by the presence of weak rocks in the fault zone rather than by high fluid pressures, analysis of rock samples from active (Holdsworth et al., 2011) and exhumed (Warr and Cox, 2001) fault zones suggests that transient fluid overpressures do occur in many fault zones and are most likely generated during coseismic faulting due to shear heating, low permeability, high water content, and low strength of clay-rich shear zones.

Whether due to mineralogy and/or fluid pressure affects, how or when stable aseismic surface creep initiates on active faults remains uncertain. The fact that creeping segments of the North Anatolian fault at Ismetpasa and the San Andreas fault in the San Francisco Bay area also rupture coseismically suggests to us that fault creep may be initiated as postseismic afterslip (Çakir et al., 2005; Schmidt et al., 2005), a mechanism that could not be confirmed previously due to the lack of pre- and post-earthquake observations on these fault sections. In this study we use space geodetic data and recent field observations along the A.D. 1999 Izmit earthquake rupture (Fig. 1) to demonstrate continuing afterslip that appears to grade into steady-state creep on a >60-km-long segment of the Izmit coseismic fault, supporting seismic slip as one of the possible mechanisms for initiating steady-state creep on mature strike-slip faults.

THE 1999 IZMIT EARTHQUAKE

The M_w 7.4 Izmit earthquake on 17 August 1999 occurred on the North Anatolian fault,

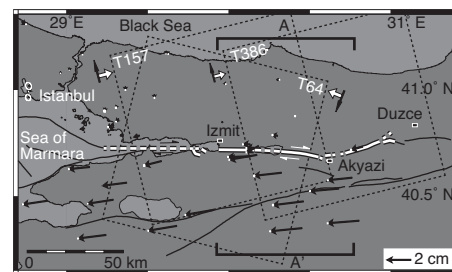


Figure 1. Map of the 1999 Izmit earthquake region (Turkey) showing the coseismic surface rupture (thick white lines), active faults (black lines), and GPS velocities (black arrows) with 95% confidence ellipses relative to Eurasia between A.D. 2002 and 2011. Dashed rectangles are frames of ERS and ENVISAT satellite images studied and are labeled in white with track numbers. White and black arrows indicate satellites' line of sight look, and flight directions, respectively. Brackets indicate location of profile in Figure 4B.

with a supershear rupture velocity (Bouchon et al., 2001) along its central segment, causing the loss of more than 18,000 people and heavy destruction in the eastern Marmara region of Turkey (Barka et al., 2002) (Fig. 1). The event was not completely unexpected because westward-migrating earthquakes that broke an ~1000-km-long section of the North Anatolian fault between 1939 and 1967 had already occurred near Izmit (e.g., Stein et al., 1997). Another large and destructive earthquake is expected to occur in the near future (with a probability of >50% over the next 30 yr) further west along the North Anatolian fault under the Sea of Marmara, 20 km south of Istanbul (Parsons, 2004). Earlier studies of postseismic deformation of Izmit using GPS and interferometric synthetic aperture radar (InSAR) measurements interpreted the surface deformation within the first few months following the event as due primarily to afterslip on and below the Izmit rupture (Bürgmann et al., 2002; Çakir et al., 2003; Ergintav et al., 2009). Later postseismic deformation has been attributed to viscoelastic relaxation of the lower crust and/or upper mantle (Hearn et al., 2009; Wang et al., 2009).

*E-mails: Ziyadin.Cakir@itu.edu.tr; semih.ergintav@tubitak.gov.tr; ozener@boun.edu.tr; dogan@yildiz.edu.tr; Ahmet.Akoglu@kaust.edu.sa; m.meghraoui@unistra.fr; reilinger@erl.mit.edu.

PRE- AND POST-EARTHQUAKE SURFACE DEFORMATION

Using the persistent scatterer InSAR (PSI) technique, we generated time series and mean radar line-of-sight (LOS) velocity maps of the surface movements in the Izmit region during ~10 yr before and after the earthquake from SAR images generated by the European Space Agency's ERS and ENVISAT satellites. We used SAR images on a descending track of ERS (track 64) and two overlapping and neighboring ascending tracks of ENVISAT (tracks 157 and 386) to investigate the pre- and post-seismic deformation fields, respectively (Fig. 1). Multi-temporal InSAR techniques such as PSI are required when studying subtle and slow deformation along active faults because they allow a reduction in the effects of noise and signal decorrelation due to atmospheric changes, digital elevation model (DEM) errors, and orbital inaccuracies by filtering in time and space, and selecting only the most coherent pixels for analysis. We processed the SAR data using the software package StaMPS with the SRTM-3 DEM for the removal of the topographic phase contribution (Hooper, 2008). We removed orbital residuals using the best-fitting plane parameters estimated by StaMPS. The detailed processing procedure can be found in Hooper (2008). Postseismic GPS data for the period between A.D. 2002 and 2011 were processed with the GAMIT/GLOBK GPS software (Herring et al., 2010).

The mean LOS velocity field from 22 SAR images on track 157, and 14 SAR images on track 386 (Fig. 2) acquired between 2002 and 2009 reveals that the Izmit-Akyazi segment that ruptured at a supershear speed during the 1999 Izmit earthquake (Bouchon et al., 2001) is now aseismically creeping (Figs. 3A and 3B). The generation of fractures with right-lateral slip on a concrete wall built across the fault south of Izmit (29.942°E, 40.72°N) in 2008 and repeated geodetic survey measurements of a nearby off-set channel wall confirm the aseismic surface slip (Fig. DR1 in the GSA Data Repository¹). Surface creep along the supershear section of the fault is evident in the postseismic radar LOS velocity field on both tracks, and can be seen as a sharp change in colors from blue to red across the fault in Figures 3A and 3B. The absence of such sharp or abrupt changes across the fault in the preseismic LOS velocity field deduced from 24 ERS SAR images acquired on track 64 between 1992 and 1999 indicates that the fault was not creeping, and was therefore locked up to the surface before the 1999 Izmit

¹GSA Data Repository item 2012322, supplementary figure showing field observations of surface creep, is available online at www.geosociety.org/pubs/ft2012.htm, or on request from editing@geosociety.org or Documents Secretary, GSA, P.O. Box 9140, Boulder, CO 80301, USA.

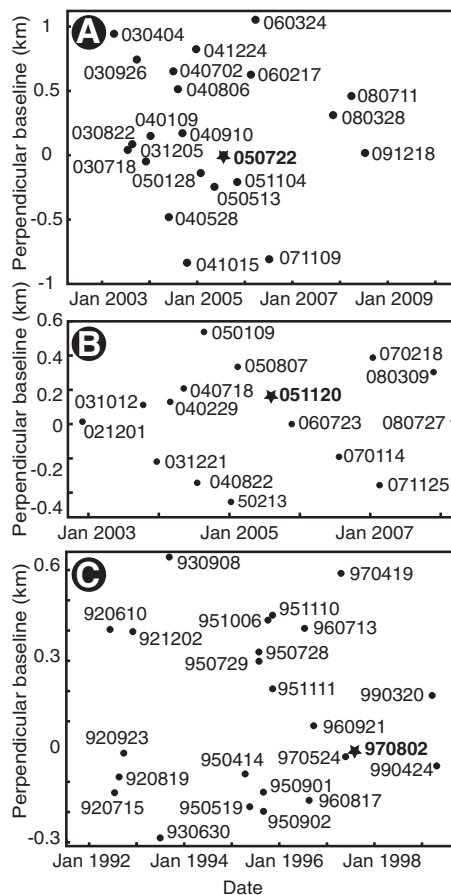


Figure 2. Baseline plot of synthetic aperture radar (SAR) images used to calculate the deformation field and time series before and after the 1999 Izmit earthquake. Plot points are labeled with date of image acquisition (yyymmdd). A: ENVISAT track 157. B: ENVISAT track 386. C: ERS track 64. Stars indicate master orbits chosen for persistent scatterer InSAR (PSI) analyses.

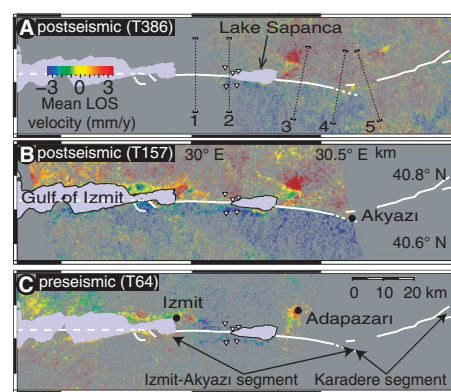


Figure 3. Surface displacements along the 1999 Izmit earthquake rupture as deduced from interferometric synthetic aperture radar (InSAR) time series. A,B: Mean line-of-sight (LOS) velocity field (denoted by colors) after the earthquake. C: Mean LOS velocity field before the earthquake. Dashed lines are locations of profiles shown in Figure 4A. White inverted triangles are GPS stations (see Fig. 5). T157—ENVISAT track 157; T386—ENVISAT track 386; T64—ERS track 64.

earthquake (Fig. 3C). The LOS velocity field on track 386 shows that surface creep is restricted to the supershear segment because there is no velocity contrast across the Karadere segment, although some aseismic slip on the Karadere segment may occur at seismogenic depths (Peng and Ben-Zion, 2006). In addition, the SAR data provide no information on possible creep along the submarine fault segment to the west in the Gulf of Izmit.

Profiles of pre- and post-seismic InSAR and GPS fault-parallel velocities plotted in Figure 4, together with surface velocities predicted by elastic screw dislocation models for creeping and non-creeping faults, better illustrate the change in fault behavior after the earthquake; postseismic surface or near-surface creep along the fault is manifested by steps at the fault in the otherwise nearly flat velocity profiles (Fig. 4A). The absence of steps in the pre-earthquake velocity profiles attests to the absence of shallow fault creep prior to the 1999 earthquake. The pattern and height of steps along the post-earthquake profiles are controlled by the locking depth and rate of aseismic creep, respectively; the steeper the step, the shallower the locking depth, and the higher the step, the higher the creep rate. Thus, while vertical jumps in profiles indicate creep reaching to the surface (i.e., zero upper locking depth), gradual rises show deeper locking depths.

MODELING

We modeled the fault-parallel InSAR velocity profiles using screw dislocations on two infinitely long and vertical faults stacked vertically in an elastic half space (Savage and Burford, 1973): one fault representing the steady-state interseismic creep below 12 km (to infinity) at a fixed rate of 27 mm/yr (Reilinger et al., 2006), and the other fault representing the shallow creeping section above. Four parameters are estimated from the profiles: creep rate, depths to the top and bottom of the creeping segment of the upper fault, and a shift in the reference point for velocity. To estimate these parameters, we use a modified bootstrap procedure with a least squares optimization algorithm with an upper bound of 27 mm/yr for the creep rate and 12 km for the depth to the bottom of the creeping section. Bootstrap standard errors and 95% confidence limits are estimated from the 500-parameter estimates. Despite some discrepancies, independent parameter estimates from the two sets of SAR data are generally broadly consistent (Figs. 5C and 5D). The creep rate increases eastward from 5 to 10 mm/yr near Izmit to the pre-earthquake, cross-fault rate of 27 ± 2 mm/yr near Lake Sapanca, diminishing to zero at the eastern end of Izmit-Akyazi segment (Fig. 5C). Although creeping depth (i.e., depth to the bottom of the creeping section of the upper fault) increases eastward from 4–5 km to 10–12 km

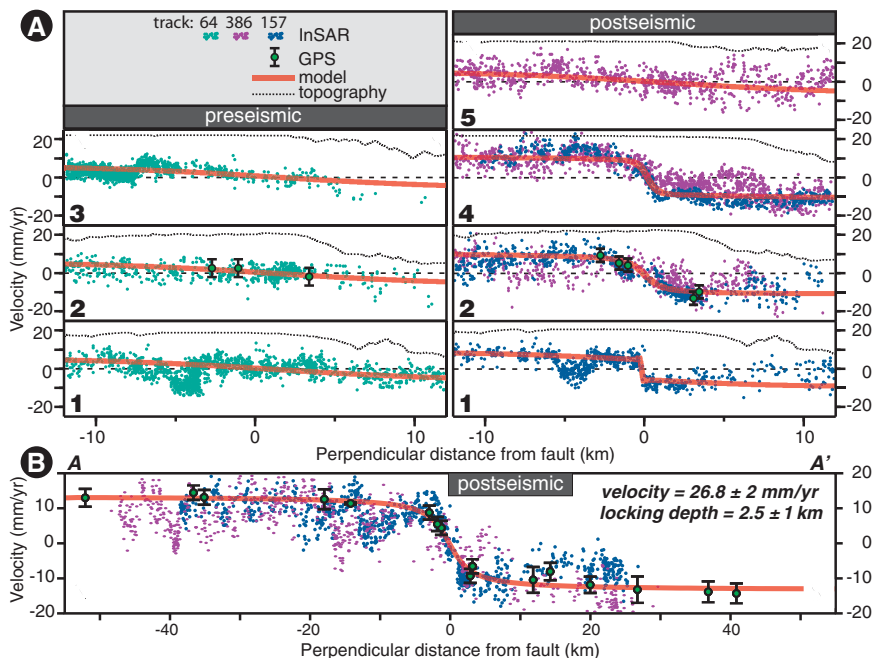


Figure 4. Velocity profiles and modeling. A: Fault-parallel horizontal velocities before (left panel) and after (right panel) the Izmit earthquake, observed and modeled along profiles perpendicular to the fault (see Fig. 3A for profile locations). B: GPS and interferometric synthetic aperture radar (InSAR) velocities plotted versus distance from fault along profile A–A' shown in Figure 1. Red curve shows best fitting model to GPS data. Model parameters are given in Figures 5C and 5D. All velocities are calculated assuming radar line-of-sight displacements are due to purely horizontal motion on an east-west-trending strike-slip fault.

(Fig. 5D), deep creep (>12 km) south of Adapazari is likely due to the non-tectonic LOS signal in the city observed in all InSAR data (Fig. 3).

DISCUSSION

Except for the first 10 km of the fault east of Izmit, aseismic creep does not appear to reach the surface although it is very shallow (mostly <1 km) (Figs. 4A [profile 1] and 5D). This may result from distributed creep and/or anelastic deformation within the less-consolidated and more-fractured surface materials, which would broaden the zone of deformation around the fault and thus mimic the effects of a fault locked at a superficial depth. In this case, the observations we present are consistent with creeping up to the surface at rates reaching the pre-earthquake cross-fault rate of 27 ± 2 mm/yr along the full ~60 km length of the Izmit-Akyazi supershear rupture segment.

The occurrence of shallow fault creep finds support from displacements along the fault monitored since the early 1990s using a near-field small-aperture GPS network west of Lake Sapanca (Fig. 5A). The slip history of the fault is illustrated in Figure 5E using the fault-parallel component of baseline change between two GPS points located ~3 km from, and on either side of, the fault which is projected on to the LOS for comparison with the InSAR time series. The GPS and InSAR measurements are in good agreement and show that rapid postseismic afterslip started immediately after the earthquake following the coseismic offset of ~3 m between the two GPS points (Barka et al., 2002). As expected, afterslip decays logarithmically with time and appears to have reached a steady-state stage over the last decade or so, indicating that fault creep continues at present and may continue for decades and possibly until late in the earthquake cycle (i.e., ~200–300 yr). To the extent that this proves to be the case, postseismic afterslip has evolved into fault creep with time.

Fault creep reaching the surface along the Hayward (San Andreas fault) and Ismetpaşa (North Anatolian fault) fault segments may have been induced in a similar way; postseismic afterslip may have evolved into long-term fault creep following the large earthquakes in A.D. 1868 (Schmidt et al., 2005) and 1944 (Çakir et al., 2005), respectively. Surface creep may have been driven initially by coseismic stress changes as postseismic afterslip, but the absence of a clear correlation between the distribution of coseismic surface slip and creep rate (Figs. 5B and 5C) suggests it is now driven by another mechanism, possibly the deep relaxation processes inferred by Hearn et al. (2009). Trapped pore-fluid overpressures in the fault zone induced by the supershear rupture propagation may also be an important mechanism for

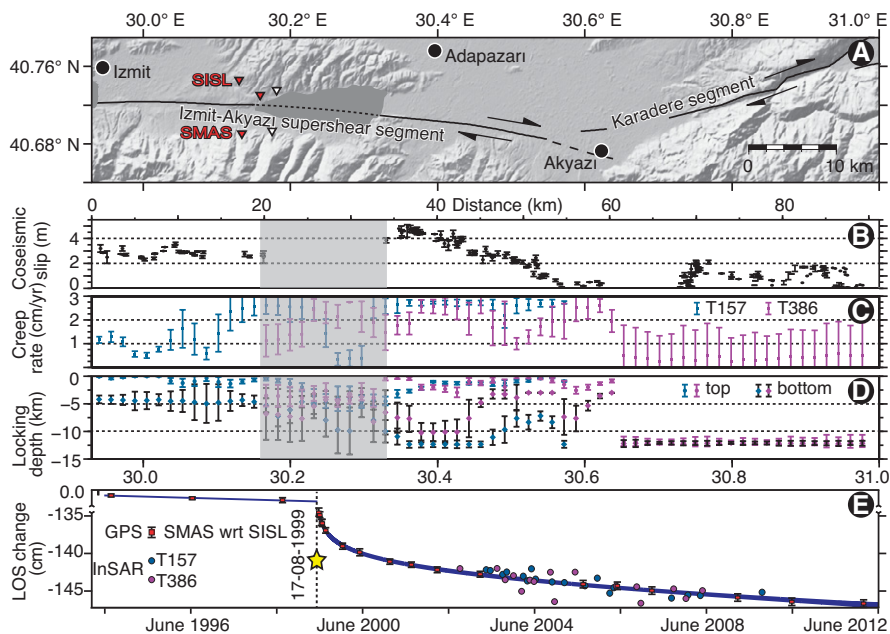


Figure 5. Slip characteristics of the Izmit fault. A: Supershear and Karadere segments of the Izmit earthquake rupture (black lines) and the Sapanca micro-GPS network (inverted triangles), with red denoting pre-earthquake stations). B: Coseismic surface slip (Emre et al., 2003). C, D: Creep rates and depths to the top and bottom of the creeping fault deduced from elastic dislocation modeling of interferometric synthetic aperture radar (InSAR) data. E: Time series of fault-parallel component of baseline change between SMAS and SISL GPS benchmarks (red squares) shown in A and postseismic InSAR data (blue and purple circles) for a nearby point. Blue curve is a fit to the GPS data of the form $a + bt + c \log(t)$ (t is time in years) with line thickness showing 95% prediction bounds. The coefficients a , b , and c inverted with a Levenberg-Marquardt inversion approach are 0.19 ± 0.7 mm, -0.54 ± 0.1 mm, and 4.66 ± 0.5 mm, respectively. Star indicates Izmit earthquake, with date shown in the form dd-mm-yyyy. Shaded sections in B–D correspond to Lake Sapanca section where parameters are not well constrained. T157—ENVISAT track 157; T386—ENVISAT track 386.

initiating fault creep behavior. Continuation of surface creep to date, however, requires unusually slow dissipation of overpressures and/or the presence of weak minerals in the fault zone.

The pattern of postseismic GPS and LOS velocities shown in Figure 4B and elastic modeling suggest that a significant amount of elastic strain has been released along the central section of the Izmit fault during the last decade, retarding stress accumulation on the fault as a whole and causing stress concentrations on locked portions of the fault, particularly at its tips. Accordingly, models of stress transfer need to include the additional changes in stress caused by aseismic fault creep that can promote or retard failure on adjacent faults. This is particularly important for the seismic gap segment of the North Anatolian fault in the Sea of Marmara south and west of Istanbul that is expected to be hit by a destructive earthquake within a couple of decades (Parsons, 2004).

CONCLUSIONS

We investigated pre- and post-earthquake surface deformation along the North Anatolian fault in the 1999 Izmit earthquake region using space geodesy and field observations. We show that shallow sections of the supershear segment of the 1999 Izmit rupture began to creep aseismically after the earthquake, initially at a rapid rate that graded into a steady-state rate comparable to its long-term, pre-earthquake slip rate. This suggests that surface creep along major strike-slip faults may be initiated as postseismic afterslip following a large earthquake. Although fault creep appears to correlate spatially with the supershear segment of the Izmit coseismic fault, a causal relationship has not been established. Further monitoring of fault movements using the GPS network in Sapanca and a recently established GPS network near Izmit will help clarify the longer-term creep behavior of this segment of the North Anatolian fault, the role of postseismic afterslip in initiating subsequent fault creep, and how these mechanisms impact estimates of stress transfer and earthquake recurrence times.

ACKNOWLEDGMENTS

InSAR data were provided by European Space Agency under Project AOTR-2436 and by the Geohazard Supersites program, and were processed at the TUBITAK ULAKBIM High Performance and Grid Computing Centre (Turkey). We thank Onur Tan and Aynur Dikbas for their field assistance, and Aral Okay, Roland Burgmann, and an anonymous reviewer for their helpful reviews. Reilinger's participation was supported by U.S. National Science Foundation grant EAR-1045487 to the Massachusetts Institute of Technology. This study is supported by TUBITAK project 107Y281.

REFERENCES CITED

- Barka, A.A., and 21 others, 2002, Surface rupture and slip distribution of the 17 August 1999 İzmit earthquake (M 7.4), North Anatolian Fault: *Bulletin of the Seismological Society of America*, v. 92, p. 43–60, doi:10.1785/0120000841.
- Bouchon, M., Bouin, M.P., Karabulut, H., Toksoz, M.N., Dietrich, M., and Rosakis, A.J., 2001, How fast is rupture during an earthquake? New insights from the 1999 Turkey earthquakes: *Geophysical Research Letters*, v. 28, p. 2723–2726, doi:10.1029/2001GL013112.
- Bürgmann, R., Ergintav, S., Segall, P., Hearn, E., McClusky, S., Reilinger, R., Woith, H., and Zschau, J., 2002, Time-dependent distributed afterslip on and deep below the İzmit earthquake rupture: *Bulletin of the Seismological Society of America*, v. 92, p. 126–137, doi:10.1785/0120000833.
- Bürgmann, R., Schmidt, D., Nadeau, R.M., d'Alessio, M., Fielding, E., Manaker, D., McEvilly, T.V., and Murray, M.H., 2000, Earthquake potential along the northern Hayward fault, California: *Science*, v. 289, p. 1178–1182, doi:10.1126/science.289.5482.1178.
- Byerlee, J.D., 1990, Friction, overpressure and fault normal compression: *Geophysical Research Letters*, v. 17, p. 2109–2112, doi:10.1029/GL017i012p02109.
- Çakir, Z., de Chabaliere, J.B., Armijo, R., Meyer, B., Barka, A., and Peltzer, G., 2003, Coseismic and early postseismic slip associated with the 1999 İzmit earthquake (Turkey), from SAR interferometry and tectonic field observations: *Geophysical Journal International*, v. 155, p. 93–110, doi:10.1046/j.1365-246X.2003.02001.x.
- Çakir, Z., Akoglu, A.M., Belabbes, S., Ergintav, S., and Meghraoui, M., 2005, Creeping along the İsmetpaşa section of the North Anatolian Fault (Western Turkey): Rate and extent from InSAR: *Earth and Planetary Science Letters*, v. 238, p. 225–234, doi:10.1016/j.epsl.2005.06.044.
- Carpenter, B.M., Marone, C., and Saffer, D.M., 2011, Weakness of the San Andreas Fault revealed by samples from the active fault zone: *Nature Geoscience*, v. 4, p. 251–254, doi:10.1038/geo1089.
- Collettini, C., Niemeijer, A., Viti, C., and Marone, C., 2009, Fault zone fabric and fault weakness: *Nature*, v. 462, p. 907–910, doi:10.1038/nature08585.
- Emre, Ö., Awata, Y., and Duman, T.Y., 2003, Surface Rupture Associated with the 17 August 1999 İzmit Earthquake: Ankara, Turkey, General Directorate of Mineral Research and Exploration, Special Publication 138.
- Ergintav, S., McClusky, S., Hearn, E.H., Reilinger, R.E., Cakmak, R., Herring, T., Ozener, H., Lenk, O., and Tari, E., 2009, Seven years of postseismic deformation following the 1999, M = 7.4 and M = 7.2, İzmit-Düzce, Turkey earthquake sequence: *Journal of Geophysical Research*, v. 114, B07403, doi:10.1029/2008JB006021.
- Hearn, E.H., McClusky, S., Ergintav, S., and Reilinger, R.E., 2009, İzmit earthquake postseismic deformation and dynamics of the North Anatolian Fault Zone: *Journal of Geophysical Research*, v. 114, B08405, doi:10.1029/2008JB006026.
- Herring, T.A., King, R.W., and McClusky, S., 2010, Introduction to GAMIT/GLOBK, Release 10.4: Cambridge, Massachusetts, Massachusetts Institute of Technology, 48 p.
- Holdsworth, R.E., van Diggelen, E.W.E., Spiers, C.J., de Bresser, J.H.P., Walker, R.J., and Bowen, L., 2011, Fault rocks from the SAFOD core samples: Implications for weakening at shallow depths along the San Andreas Fault, California: *Journal of Structural Geology*, v. 33, p. 132–144, doi:10.1016/j.jsg.2010.11.010.
- Hooper, A., 2008, A multi-temporal InSAR method incorporating both persistent scatterer and small baseline approaches: *Geophysical Research Letters*, v. 35, L16302, doi:10.1029/2008GL034654.
- Lockner, D.A., Morrow, C., Moore, D., and Hickman, S., 2011, Low strength of deep San Andreas fault gouge from SAFOD core: *Nature*, v. 472, p. 82–85, doi:10.1038/nature09927.
- Parsons, T., 2004, Recalculated probability of M \geq 7 earthquakes beneath the Sea of Marmara, Turkey: *Journal of Geophysical Research*, v. 109, B05304, doi:10.1029/2003JB002667.
- Peng, Z., and Ben-Zion, Y., 2006, Temporal changes of shallow seismic velocity around the Karadere-Düzce branch of the North Anatolian fault and strong ground motion: *Pure and Applied Geophysics*, v. 163, p. 567–600, doi:10.1007/s00024-005-0034-6.
- Reilinger, R.E., and 20 others, 2006, GPS constraints on continental deformation in the Africa-Arabia-Eurasia continental collision zone and implications for the dynamics of plate interactions: *Journal of Geophysical Research*, v. 111, V05411, doi:10.1029/2005JB004051.
- Savage, J.C., and Burford, R.O., 1973, Geodetic determination of relative plate motion in central California: *Journal of Geophysical Research*, v. 78, p. 832–845.
- Schleicher, A.M., van der Pluijm, B.A., and Warr, L.N., 2010, Nano-coatings of clay and creep of the San Andreas Fault at Parkfield, California: *Geology*, v. 38, p. 667–670, doi:10.1130/G31091.1.
- Schmidt, D.A., Bürgmann, R., Nadeau, R.M., and d'Alessio, M., 2005, Distribution of aseismic slip rate on the Hayward fault inferred from seismic and geodetic data: *Journal of Geophysical Research*, v. 110, B08406, doi:10.1029/2004JB003397.
- Stein, R.S., Barka, A.A., and Dietrich, J.H., 1997, Progressive failure on the North Anatolian Fault since 1939 from earthquake stress triggering: *Geophysical Journal International*, v. 128, p. 594–604, doi:10.1111/j.1365-246X.1997.tb05321.x.
- Wang, L., Wang, R., Roth, F., Enescu, B., Hainzl, S., and Ergintav, S., 2009, Afterslip and viscoelastic relaxation following the 1999 M7.4 İzmit earthquake from GPS measurements: *Geophysical Journal International*, v. 178, p. 1220–1237, doi:10.1111/j.1365-246X.2009.04228.x.
- Warr, L.N., and Cox, S., 2001, Clay mineral transformations and weakening mechanisms along the Alpine fault, New Zealand, *in* Holdsworth, R.E., Strachan, R.A., Magloughlin, J.F., and Knipe, R.J., eds., *The nature and tectonic significance of fault zone weakening*: London, Geological Society (London) Special Publication, v. 186, p. 85–101.

Manuscript received 13 April 2012

Revised manuscript received 5 June 2012

Manuscript accepted 7 June 2012

Printed in USA